Available online at www.sciencedirect.com
ScienceDirect
Optics Communications 266 (2006) 660–668
OPTICS COMMUNICATIONS
www.elsevier.com/locate/optcom

# Dynamics and interaction of pulses in the modified Manakov model

Eduard N. Tsoy *, Nail Akhmediev

*Optical Sciences Group, Research School of Physical Sciences and Engineering, The Australian National University, Canberra, ACT 0200, Australia*

Received 22 December 2005; received in revised form 10 April 2006; accepted 8 May 2006

**Abstract**

The two-component vector nonlinear Schrödinger equation, with mixed signs of the nonlinear coefficients, is considered. This equation is integrable by the inverse scattering transform method. The evolution of a single pulse and interaction of pulses are studied. It is shown that the dynamics of a single pulse is reduced to the scalar nonlinear Schrödinger equation of focusing or defocusing type, depending on the initial parameters. It is found that the interaction of pulses results in the appearance of additional solitons and bound states of several solitons. The asymptotic field profile in the non-soliton regime is also obtained.


*PACS:* 05.45.Yv; 42.65.Tg

*Keywords:* Coupled nonlinear Schrödinger equations; Vector solitons; The Manakov system; Integrable systems

## 1. Introduction

A set of coupled nonlinear Schrödinger (NLS) equations is a basic model for various physical processes [1]. For example, it describes the propagation of a light beam with arbitrary polarization in a self-focusing medium [2], the continuum limit of the one-dimensional Hubbard model [3], the averaged dynamics of optical pulses in dispersion-managed fibers [4], and the dynamics of a Bose–Einstein condensate consisting of two kinds of atoms [5,6]. In many cases, as a result of the dynamics, the vector field forms a bound state of scalar solitary waves. The latter can be either a pulse-like wave, with zero values of a component at $x \to \infty$ (*bright* solitons), or a localized dip on a constant background (*dark* solitons). We recall that bright and dark solitons are the fundamental modes of the scalar focusing and defocusing NLS equations, respectively.

Let us consider a set of coupled NLS equations in the following form:

$$\begin{aligned} &i\psi_{1,Z} + D\psi_{1,XX} + 2\gamma(\alpha_{11}|\psi_1|^2 + \alpha_{12}|\psi_2|^2)\psi_1 = 0,\\ &i\psi_{2,Z} + D\psi_{2,XX} + 2\gamma(\alpha_{21}|\psi_1|^2 + \alpha_{22}|\psi_2|^2)\psi_2 = 0, \end{aligned} \tag{1}$$

where $\psi_1(X,Z)$ and $\psi_2(X,Z)$ are the envelopes of the field components, $X$ and $Z$ are the spatial and evolutional variables, respectively, $\gamma$ and $\alpha_{j,k}$ are the nonlinearity parameters, and the dispersion coefficient $D$ is taken to be the same in the both components. It has been found [7] that the system (1) is integrable by the inverse scattering transform (IST) method, if either $\alpha_{11} = \alpha_{12} = \alpha_{21} = \alpha_{22}$, or $\alpha_{11} = \alpha_{21} = -\alpha_{12} = -\alpha_{22}$. Assuming such relations between the coefficients $\alpha_{jk}$ and taking $|\alpha_{jk}| = 1$, one can write Eqs. (1) in dimensionless form as the generalized Manakov system [2]:

$$\begin{aligned} &iq_{1,z} + q_{1,xx} + 2(|q_1|^2 + \sigma|q_2|^2)q_1 = 0,\\ &iq_{2,z} + q_{2,xx} + 2(|q_1|^2 + \sigma|q_2|^2)q_2 = 0, \end{aligned} \tag{2}$$

where $z = Z/Z_c$, $x = X/X_c$ and $q_j = \psi_j/\psi_c$, and $\sigma = \pm 1$. Here $Z_c = X_c^2/D$, $\psi_c = (D/\gamma)^{1/2}/X_c$ and $X_c$ is the characteristic scale in $X$, e.g. the initial pulse width.

Recent studies [1,2,8,9] have mostly concentrated on the case $\sigma = 1$, which we call the *conventional* Manakov (CM) equations. There are a few works relating to the case

* Corresponding author. Address: Physical-Technical Institute of the Uzbek Academy of Sciences, Mavlyanov Street, 2-B, Tashkent 700084, Uzbekistan. Tel.: +998 711354338; fax: +998 711354291.
*E-mail address:* etsoy@physic.uzsci.net (E.N. Tsoy).

0030-4018/$ - see front matter © 2006 Elsevier B.V. All rights reserved.
doi:10.1016/j.optcom.2006.05.017

$\sigma = -1$ (see papers [7,10,11] and references therein), which we refer to as the *modified* Manakov (MM) model. The integrability of Eq. (2) with $\sigma = -1$ was demonstrated in Refs. [7,10]. Exact solutions, corresponding to pairs of bright and dark scalar solitons are given in Ref. [10]. The known solutions, along with the new ones, are listed in Ref. [11].

In real physical systems described by Eqs. (1), it is usually assumed that the cross-phase modulation coefficients are equal, i.e. $\alpha_{12} = \alpha_{21}$. In order to obtain such a case in Eq. (2), one can consider the fields $q_1$ and $q_2^\star$ (the complex conjugate of $q_2$). Then for $\sigma = -1$, the component $q_1$ operates in the anomalous dispersion region, while $q_2^\star$ is in the normal dispersion one. The self-modulation coefficients are positive, while the cross-phase modulation coefficients are negative. Such a set of the coefficients can be realized in optical materials with quadratic nonlinearity. It has been shown [12] that the wave–wave interaction with a large phase mismatch is described by equations similar to Eqs. (1). The model (2) with $\sigma = -1$ can also be obtained as the continuous limit of some discrete systems or in the description of systems with periodic modulation of parameters. A first example is the dynamics of vector solitons in waveguide arrays [13–16]. Another relevant system is a chain of drops of a binary Bose–Einstein condensate (BEC) trapped in an optical lattice [17–21]. An appropriate description of periodic or discrete systems can be implemented in terms of modulated Bloch waves (see e.g. [16]). Choosing different carrier frequencies for the components, one can obtain dispersion coefficients with opposite signs. The nonlinear parameters can be tuned by using appropriate media or by applying external fields. In the case of a BEC, the values and signs of the nonlinear coefficients can be changed by an external magnetic field (the Feschbach resonance). Then, the large-scale excitations are described by Eqs. (2) with $\sigma = -1$.

In the present paper we study the evolution of pulses in the modified Manakov model, Eq. (2) with $\sigma = -1$. The paper is organized as follows. In Section 2, we outline the IST method for Eqs. (2). In Section 3, we consider the dynamics of a single pulse and the interaction of two pulses. Using IST theory we obtain equations which describe the asymptotic state of the system. Section 4 summarizes the main results of the paper.

## 2. The inverse scattering transform method

In this section, we give an overview of the IST method for Eqs. (2) [7,10]. We follow the approach developed in Refs. [8,22] for the CM model and for the vector NLS equation, respectively. We write all the equations in a form that can be applied both to the CM and MM models.

We start from the set of the two coupled NLS equations (2). In the rest of the paper we mainly consider the case $\sigma = -1$. However, parameter $\sigma$ is retained explicitly in the equations, so that the results will be applicable to both cases, viz. $\sigma = 1$ and $\sigma = -1$. The system (2) is a particular case of a set of matrix equations

$$\begin{aligned} \mathrm{i}\mathbf{Q}_z &= \mathbf{Q}_{xx} - 2\mathbf{QRQ}, \\ \mathrm{i}\mathbf{R}_z &= -\mathbf{R}_{xx} + 2\mathbf{RQR}, \end{aligned} \tag{3}$$

which is integrable by the inverse scattering transform (IST) method (see overview in Ref. [22]). Here $\mathbf{Q}$ is an $N \times M$ matrix and $\mathbf{R}$ is an $M \times N$ matrix. Eqs. (3) reduce to the MM system if $N = 1$, $M = 2$, and $\mathbf{R} = -\mathbf{J}_0\mathbf{Q}^\dagger$, and to the CM equations if $N = 1$, $M = 2$, and $\mathbf{R} = -\mathbf{Q}^\dagger$, where

$$\mathbf{J}_0 = \begin{pmatrix} 1 & 0 \\ 0 & -1 \end{pmatrix},$$

and † means Hermitian conjugate.

The integrability of Eqs. (2) means, in particular, that there exist two linear equations [10]

$$f_x = Uf, \quad f_z = Vf, \tag{4}$$

so that the compatibility condition

$$U_z - V_x + [U, V] = 0 \tag{5}$$

results in Eqs. (2). Here $f$ is a three-component vector, $U$ and $V$ are $3 \times 3$ matrices, and $[U, V] \equiv UV - VU$. Eqs. (4) can be written explicitly in the following form [10]

$$\begin{aligned} f_{1,x} + \mathrm{i}\lambda f_1 &= q_1 f_2 + q_2 f_3, \\ f_{2,x} - \mathrm{i}\lambda f_2 &= -q_1^\star f_1, \\ f_{3,x} - \mathrm{i}\lambda f_3 &= -\sigma q_2^\star f_1, \end{aligned} \tag{6}$$

and

$$\begin{aligned} f_{1,z} &= [-2\mathrm{i}\lambda^2 + \mathrm{i}(|q_1|^2 + \sigma|q_2|^2)]f_1 + (2\lambda q_1 + \mathrm{i}q_{1,x})f_2 \\ &\quad + (2\lambda q_2 + \mathrm{i}q_{2,x})f_3, \\ f_{2,z} &= (-2\lambda q_1^\star + \mathrm{i}q_{1,x}^\star)f_1 + (2\mathrm{i}\lambda^2 - \mathrm{i}|q_1|^2)f_2 - \mathrm{i}q_1^\star q_2 f_3, \\ f_{3,z} &= \sigma(-2\lambda q_2^\star + \mathrm{i}q_{2,x}^\star)f_1 - \mathrm{i}\sigma q_1 q_2^\star f_2 + (2\mathrm{i}\lambda^2 - \mathrm{i}\sigma|q_2|^2)f_3, \end{aligned} \tag{7}$$

where $\lambda$ is the spectral parameter. The IST method provides detailed information about the system (see e.g. Ref. [23]), including an infinite set of invariant quantities, families of exact solutions and characteristics of the long-time behavior.

The initial-value problem for Eq. (2) can be solved, in principle, by using Eqs. (6) and (7) (see e.g. Refs. [22,23]). To do this, one first needs to solve the direct scattering problem (6) with functions $q_1(x, 0)$ and $q_2(x, 0)$. The solution gives the scattering data at $z = 0$. The evolution, in $z$, of the scattering data is determined from Eqs. (7). Finally, one needs to reconstruct the functions $q_1(x, z)$ and $q_2(x, z)$ from the scattering data at time $z$ by solving the inverse scattering problem. Below, in this section, we present the main equations of the IST method for Eqs. (2).

Let $\mathbf{\Phi}$ and $\mathbf{\Psi}$ be the solution matrices [2,8] for Eq. (6) with the following boundary conditions, respectively

$$\mathbf{\Phi}(x\to-\infty,\lambda)=\begin{pmatrix}e^{-i\lambda x}&0&0\\0&e^{i\lambda x}&0\\0&0&e^{i\lambda x}\end{pmatrix},$$
$$\mathbf{\Psi}(x\to+\infty,\lambda)=\begin{pmatrix}e^{-i\lambda x}&0&0\\0&e^{i\lambda x}&0\\0&0&e^{i\lambda x}\end{pmatrix}. \quad (8)$$

Then the scattering matrix $S=[s_{ij}]$ is defined as [2,8]

$$\mathbf{\Phi}(x,\lambda)=\mathbf{\Psi}(x,\lambda)S^{T}, \quad (9)$$

where superscript T means the matrix transpose. One can show that matrix $S$ is unitary for real $\lambda$, i.e. $S^{\dagger}S=I$, where $I$ is the unit matrix.

The scattering data include the continuous spectrum and the bound-state (discrete) spectrum (see e.g. Refs. [22,23]). The former is related to the elements of the scattering matrix as $\rho_1(\lambda)=s_{12}(\lambda)/s_{11}(\lambda)$ and $\rho_2(\lambda)=s_{13}(\lambda)/s_{11}(\lambda)$ for real $\lambda$. The latter consists of $N$ zeros $\lambda_n$, $n=1,2,\ldots,N$, of the element $s_{11}(\lambda)$ in the upper half of the complex $\lambda$-plane, and a set of normalization constants $C_{1n}=s_{12}(\lambda_n)/s'_{11}(\lambda_n)$ and $C_{2n}=s_{13}(\lambda_n)/s'_{11}(\lambda_n)$, where $s'_{11}\equiv ds_{11}/d\lambda$. From Eq. (7) and the definition of $S$, one can find (c.f. Refs. [8,22]) the evolution of the scattering matrix elements, so that, for real $\lambda$

$$\partial_z s_{11}(\lambda)=0,\quad \partial_z\rho_1=4i\lambda^2\rho_1,\quad \partial_z\rho_2=4i\lambda^2\rho_2, \quad (10)$$

and for bound states

$$\partial_z\lambda_n=0,\quad \partial_z C_{1n}=4i\lambda_n^2 C_{1n},\quad \partial_z C_{2n}=4i\lambda_n^2 C_{2n}. \quad (11)$$

The inverse scattering problem for the set (6) requires us to solve the following set of linear integral equations (c.f. Refs. [8,22]):

$$F_1(x,\lambda)=\mathbf{e}_1+\sum_{n=1}^{N}\frac{e^{2i\lambda_n x}}{(\lambda-\lambda_n)}[F_{2n}(x)C_{1n}+F_{3n}(x)C_{2n}]+\frac{1}{2\pi i}\int_{-\infty}^{\infty}\frac{e^{2i\xi x}}{\xi-(\lambda-i0)}[F_2(x,\xi)\rho_1(\xi)+F_3(x,\xi)\rho_2(\xi)]\,d\xi,$$
$$(F_2(x,\lambda),F_3(x,\lambda))=(\mathbf{e}_2,\mathbf{e}_3)-\sum_{n=1}^{N}\frac{e^{-2i\lambda_n^{\star}x}}{(\lambda-\lambda_n^{\star})}F_{1n}(x)(C_{1n}^{\star},\sigma C_{2n}^{\star})+\frac{1}{2\pi i}\int_{-\infty}^{\infty}\frac{e^{-2i\xi x}}{\xi-(\lambda+i0)}F_1(x,\xi)\times(\rho_1^{\star}(\xi),\sigma\rho_2^{\star}(\xi))\,d\xi, \quad (12)$$

where $F_{1n}(x)=F_1(x,\lambda_n^{\star})$, $(F_{2n}(x),F_{3n}(x))=(F_2(x,\lambda_n),F_3(x,\lambda_n))$, $n=1,\ldots,N$, $\mathbf{e}_1=(1,0,0)^T$, $\mathbf{e}_2=(0,1,0)^T$, and $\mathbf{e}_3=(0,0,1)^T$. To close the system, one needs to add equations for $F_{kn}(x)$. These can be obtained by evaluating the first of Eq. (12) at $\lambda=\lambda_n^{\star}$ and the second one at $\lambda=\lambda_n$. Then the solutions of Eq. (2) are found from

$$(q_1(x,z),q_2(x,z))=-2i\sum_{n=1}^{N}e^{-2i\lambda_j^{\star}x}[\mathbf{e}_1^{T}F_{1n}(x)](C_{1j}^{\star},\sigma C_{2j}^{\star})-\frac{1}{\pi}\int_{-\infty}^{\infty}e^{-2i\xi x}[\mathbf{e}_1^{T}F_1(x,\xi)](\rho_1^{\star}(\xi),\sigma\rho_2^{\star}(\xi)\,d\xi, \quad (13)$$

where $[\mathbf{e}_1^{T}F]$ gives the first element of the vector $F$.

If an initial condition for Eqs. (2) is taken such that the scattering data consist of the discrete spectrum only, i.e. $\rho_1(\lambda)=\rho_2(\lambda)=0$, then Eq. (12) turn into a set of algebraic equations

$$F_{1j}(x)=\mathbf{e}_1+\sum_{n=1}^{N}\frac{e^{2i\lambda_n x}}{(\lambda_j^{\star}-\lambda_n)}[F_{2n}(x)C_{1n}+F_{3n}(x)C_{2n}],$$
$$(F_{2j}(x),F_{3j}(x))=(\mathbf{e}_2,\mathbf{e}_3)-\sum_{n=1}^{N}\frac{e^{-2i\lambda_n^{\star}x}}{(\lambda_j-\lambda_n^{\star})}F_{1n}(x)(C_{1n}^{\star},\sigma C_{2n}^{\star}), \quad (14)$$

where $j=1,\ldots,N$. By solving this set of equations, a general N-soliton solution for Eq. (2) can be found. If there is only one zero, $\lambda_1=\xi+i\eta$ of $s_{11}(\lambda)$, then Eqs. (11), (13) and (14) result in a one-soliton solution (c.f. Refs. [8,22]):

$$q_1=2\eta p_1\,\mathrm{sech}y\exp(i\theta),\qquad q_2=2\eta p_2\,\mathrm{sech}y\exp(i\theta), \quad (15)$$

where

$$y=2\eta(x+4\xi z)-\log\left(\frac{\beta_0}{2\eta}\right),\quad \theta=4(\eta^2-\xi^2)z-2\xi x,$$
$$p_1=-iC_{11}^{\star}(0)/\beta_0,\quad p_2=-i\sigma C_{21}^{\star}(0)/\beta_0,$$
$$\beta_0=[|C_{11}(0)|^2+\sigma|C_{21}(0)|^2]^{1/2}.$$

The real (imaginary) part of the zero $\lambda_1$ is related to the soliton velocity (amplitude or inverse width).

If an initial condition decreases sufficiently quickly at $x\to\pm\infty$, then the solution evolves into a set of solitons and linear waves ("radiation") [1,22,23]. The latter decreases in amplitude and spreads in space. Therefore, in many cases, and particularly when the real parts of the zeros, $\lambda_n$, are different, the field consists of a set of well-separated solitons in the form of Eq. (15). However, the evolution of the continuous spectrum is also important, especially if the initial conditions are such that solitons are not generated.

## 3. Dynamics of pulses

Let us now study the dynamics of a single pulse and of a pair of them. For simplicity, we consider pulses of rectangular shape, since this allows us to solve the problem analytically. We will be interested only in asymptotic behavior at large $z$. Since the spectral parameters for the continuous and discrete spectra, $\lambda$ and $\lambda_n$, do not depend on $z$, it is sufficient to solve only the direct scattering problem equation (6). We use [c.f. Eqs. (8) and (9)] as boundary conditions

$$\begin{pmatrix}f_1\\f_2\\f_3\end{pmatrix}=\begin{pmatrix}1\\0\\0\end{pmatrix}e^{-i\lambda x}\quad \text{at } x\to-\infty,$$
$$\begin{pmatrix}f_1\\f_2\\f_3\end{pmatrix}=\begin{pmatrix}s_{11}e^{-i\lambda x}\\s_{12}e^{i\lambda x}\\s_{13}e^{i\lambda x}\end{pmatrix}\quad \text{at } x\to+\infty, \quad (16)$$

because the scattering data can be found from these three elements, $s_{11}$, $s_{12}$, and $s_{13}$, of the scattering matrix.

Now we introduce the norm $I(q_1,q_2)\equiv|q_1|^2+\sigma|q_2|^2$, which will play an important role in the further analysis. For the MM model, this parameter corresponds to the difference between the component intensities, while for the CM system, it represents the total intensity of the field. Also note that, for *real* $q_1(x,0)$ and $q_2(x,0)$, if $\lambda$ is an eigenvalue of Eq. (6), then $-\lambda^\star$ is also an eigenvalue. This means that for real potentials, eigenvalues migrate to the upper half of $\lambda$-plane by crossing the real axis either along the imaginary axis, or in pairs with opposite values of their real parts.

If $I$ is smaller than a certain threshold value, then no solitons appear (see Section 3.1). In order to describe the pulse dynamics in this case, one should obtain the parameters $\rho_1$ and $\rho_2$, solve Eq. (12) for $F_1$, $F_2$, and $F_3$, and then find the field from Eq. (13). Fortunately, the asymptotic state of the field at $z\to\infty$ can be found easily from the coefficient $s_{11}(\lambda)$ (c.f. Ref. [23]). Similarly to the NLS equation [23], in the absence of solitons, the solution of the Manakov equations at $z\to\infty$ can be written in a self-similar form as

$$\begin{aligned} q_1(x,z)&\approx z^{-1/2}y_1(Y)\exp[\mathrm{i}\theta(Y,z)+\mathrm{i}\phi_1(Y)],\\ q_2(x,z)&\approx z^{-1/2}y_2(Y)\exp[\mathrm{i}\theta(Y,z)+\mathrm{i}\phi_2(Y)],\end{aligned} \tag{17}$$

where

$$\theta(Y,z)=z\left[\frac{Y^2}{4}+2[y_1^2(Y)+\sigma y_2^2(Y)]\frac{\log z}{z}\right],\quad Y=x/z.$$

Functions $y_1(Y)$, $y_2(Y)$, $\phi_1(Y)$ and $\phi_2(Y)$ are slowly varying functions, therefore the solution Eq. (17) represents a smooth variation of the plane wave solution. The norm $I$ of the field at $z\to\infty$ is related to $s_{11}(\lambda)$ by:

$$\begin{aligned} I&=|q_1(x,z)|^2+\sigma|q_2(x,t)|^2\approx\frac{1}{z}(|y_1(Y)|^2+\sigma|y_2(Y)|^2)\\ &\approx-\frac{1}{4\pi z}\log\left|s_{11}\left(-\frac{x}{4z}\right)\right|^2\end{aligned} \tag{18}$$

### 3.1. Single pulse

We consider an initial condition in the form of a single rectangular pulse ($j=1,2$):

$$q_j(x,0)=\begin{cases}Q_j\exp(2\mathrm{i}vx), & x=[x_1,x_2],\\ 0, & \text{otherwise},\end{cases} \tag{19}$$

where $Q_1$ and $Q_2$ are complex constants and $v$ is real. It is clear that Eqs. (2), with initial condition (19), are reduced to the scalar NLS equation. Depending on the values of $Q_1$ and $Q_2$, the corresponding NLS equation can be either focusing or defocusing. We present the results for a single pulse in order to show how one can control the pulse dynamics by changing the initial polarization.

For this initial condition, we define the parameter $I_0=I(z=0)=|Q_1|^2+\sigma|Q_2|^2$, which is used below. The solution of Eqs. (6) with the potential (19) and boundary conditions (16) gives (c.f. Ref. [2])

$$\begin{aligned} s_{11}(\lambda)&=\mathrm{e}^{\mathrm{i}(\lambda+v)w}\left[\cos(\kappa w)-\frac{\mathrm{i}(\lambda+v)}{\kappa}\sin(\kappa w)\right],\\ s_{12}(\lambda)&=-\mathrm{e}^{-\mathrm{i}(\lambda+v)(x_1+x_2)}\frac{Q_1^\star}{\kappa}\sin(\kappa w),\\ s_{13}(\lambda)&=-\sigma\mathrm{e}^{-\mathrm{i}(\lambda+v)(x_1+x_2)}\frac{Q_2^\star}{\kappa}\sin(\kappa w),\end{aligned} \tag{20}$$

where $\kappa^2=(\lambda+v)^2+I_0$, $w=x_2-x_1$. The scattering coefficients in Eq. (20) have the same form for $\sigma=1$ and $\sigma=-1$. Therefore, provided that $I_0>0$, one can directly use the results of paper [2], which were obtained for the CM equations, for the MM system. They can be summarized as follows [2]:

(i) For the case $v=0$, which is applicable for items (i)–(iv), all zeros of $s_{11}(\lambda)=0$ in the upper half-plane are pure imaginary, $\lambda_n=\mathrm{i}\eta_n$. This means that the velocities of emerging solitons are equal to zero [c.f. Eq. (15)].
(ii) The number $N_S$ of zeros, or the number of solitons, depends only on the product $I_0^{1/2}w$, $I_0>0$. It is given by $N_S=\mathrm{int}[I_0^{1/2}w/\pi+1/2]$, where int[...] denotes the integer part of the argument. The parameters of the solitons, found from $\lambda_n$ and Eq. (15), depend on both $w$ and $I_0$.
(iii) If $0<I_0^{1/2}w<\pi/2$, then no solitons appear, so that all initial energy is transformed into radiation.
(iv) If $\pi/2<I_0^{1/2}w<3\pi/2$, then only one soliton emerges, while if $I_0^{1/2}w>3\pi/2$, the asymptotic field represents a bound state of $N_S$ solitons, $N_S\geqslant 2$.
(v) If $v\neq 0$, then the zeros of $s_{11}(\lambda)$ have the same real parts, $\lambda_n=-v+\mathrm{i}\eta_n$, so that all emerging solitons move with the same velocity, $4v$.

The values $I_0<0$ are specific to the MM system. The initial potential with such parameters results in only a continuous spectrum of the scattering problem (6), so that the pulse will decay dispersively and no solitons will appear. In this range of $I_0$, the defocusing component of the field dominates, and this prevents the creation of bright solitons. Fig. 1a shows the dependence of the relative norm $\bar{I}\equiv I/I(Y=0)$ multiplied by $z$ on $Y=x/z$, as found from(20) and (18). One can see that these profiles are similar to sinc function, which is an asymptotic state of the linear Schrödinger equation with the initial condition (19). Numerical simulations of the MM Eqs. (2) show that the self-similar profile is formed quickly, especially when $|Q_2|\gg|Q_1|$. The value of the peak norm, $I(Y=0)$, as a function of $|Q_2|$, is presented in Fig. 1b. A comparison of the results for $z=1$ and $z=10$ shows that Eq. (18) applies, starting from $z\sim 1$. The agreement between the numerical simulations and the theoretical prediction is quite good. Minor deviations indicate that the asymptotic state has not been reached by that time.

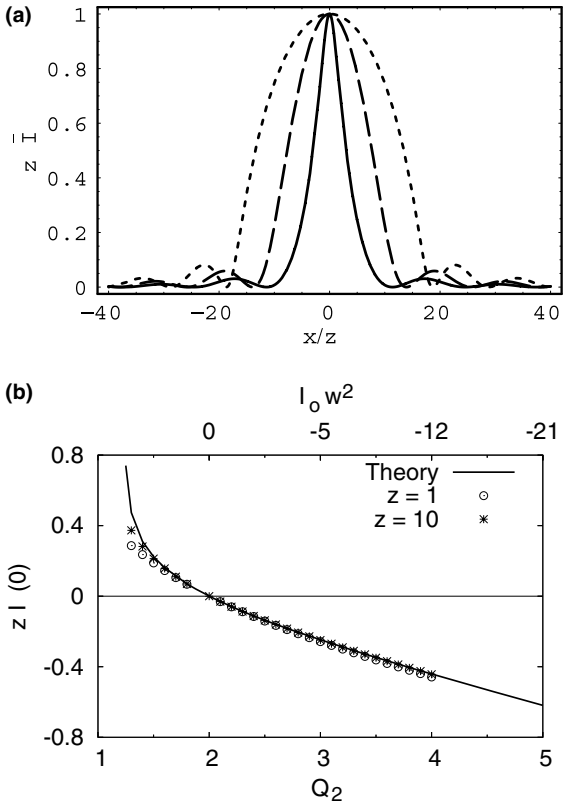


Fig. 1. Parameters of the asymptotic field for a single-pulse initial condition (19) with $Q_1 = 2$, $w = 1$ and different values of $Q_2$: (a) the relative norm $\bar{I}$, found from Eqs. (20) and (18), and multiplied by $z$, as a function of $x/z$; $Q_2 = 1.5$ (solid line), $Q_2 = 2.5$ (long dashed line) $Q_2 = 4$ (short dashed line). (b) The amplitude $I(0)$ of the norm multiplied by $z$ as a function of $Q_2$. The line is calculated using Eqs. (20) and (18), while the points are a result of numerical simulations of Eqs. (2), and the circles (stars) correspond to $z = 1$ ($z = 10$).

To summarize, in this section we have shown that if $I_0 w^2 > \pi^2/4$, then the initial condition (19) evolves into $N_S$ solitons (and radiation). The parameters of the solitons are found from the zeros of $s_{11}(\lambda)$ given by Eq. (20). As was mentioned, the MM system with initial condition (19), reduces to the *scalar* focusing NLS equation, provided that $I_0 w^2 > \pi^2/4$. A detailed study can be found in Ref. [23], for example. If $I_0 w^2 < \pi^2/4$, the initial pulse transforms into radiation only, and the distribution of the field is described asymptotically according to Eqs. (18) and (20). Therefore, if the larger amount of energy is in the first component, $|Q_1| > |Q_2|$, then the system behaves like the scalar focusing NLS equation, while if $|Q_1| < |Q_2|$, it corresponds to the defocusing case. As we will see in the next section, this conclusion does not apply to the interaction of pulses. On the other hand, we have shown that one can control the parameters of the emerging solitons by changing the initial amplitude of the second component. Large values of $Q_2$ suppress the creation of solitons.

Let us estimate the parameters in dimensional units. To our knowledge there are no experiments corresponding to the MM system. However, as mentioned in Section 1, this system can be realized in an array of 1D waveguides. Therefore, we adopt parameters close to those used in experiments on waveguide arrays [13], namely, that the array period along $x$-axis $d = 5$ μm, the coupling constant between adjacent waveguides $C = 1000\ \mathrm{m}^{-1}$ and the nonlinear coefficient $\gamma = 5\ \mathrm{m}^{-1}\ \mathrm{W}^{-1}$. Then the diffraction coefficient in Eq. (1) is found to be $D \approx C\, d^2 = 2.5 \times 10^{-8}$ m. Let the initial beam width $w_{\mathrm{in}} = 25$ μm, and the characteristic scale $X_c = w_{\mathrm{in}}$. Then the power and the propagation distance scales are $I_c \equiv |\psi_c|^2 = 8$ W and $Z_c = 2.5$ cm, respectively. The threshold value of the peak power $I_{\mathrm{th}}$ for the creation of a soliton is defined as $I_{\mathrm{th}} = (\pi^2/4) I_c \approx 20$ W.

### 3.2. Interaction of pulses

In this section, we study the interaction of two pulses. We take two rectangular pulses separated by the distance $L \equiv x_3 - x_2$ as the initial condition:

$$q_j(x,0) = \begin{cases} Q_{ja} \exp(2\mathrm{i} v_a x), & x = [x_1, x_2], \\ Q_{jb} \exp(2\mathrm{i} v_b x), & x = [x_3, x_4], \\ 0, & \text{otherwise}, \end{cases} \tag{21}$$

where $Q_{ja}$ and $Q_{jb}$ are complex constants, $j = 1, 2$, $v_a$ and $v_b$ are real, $x_1 \leqslant x_2 \leqslant x_3 \leqslant x_4$, and the indices $a$ and $b$ refer to the first and second pulses, respectively. Then the solution of the direct scattering problem (6) gives (see also Ref. [9])

$$\begin{aligned} s_{11}(\lambda) = {} & \mathrm{e}^{\mathrm{i}(\lambda+v_a)w_a}\, \mathrm{e}^{\mathrm{i}(\lambda+v_b)w_a}\, \frac{\sin(\kappa_a w_a)\sin(\kappa_b w_b)}{\kappa_a \kappa_b} \\ & \times \{[\kappa_a \cot(\kappa_a w_a) - \mathrm{i}(\lambda + v_a)][\kappa_b \cot(\kappa_b w_b) \\ & - \mathrm{i}(\lambda + v_b)] - (Q_{1a}^{\star} Q_{1b} + \sigma Q_{2a}^{\star} Q_{2b})\, \mathrm{e}^{-2\mathrm{i}(\lambda+v_a)x_2} \\ & \times \mathrm{e}^{2\mathrm{i}(\lambda+v_b)x_3}\}, \end{aligned} \tag{22}$$

where $\kappa_\alpha^2 = \lambda^2 + |Q_{1\alpha}|^2 + \sigma |Q_{2\alpha}|^2 = \lambda^2 + I_{0\alpha}$, $\alpha = a$ or $b$, $w_a = x_2 - x_1$ and $w_b = x_4 - x_3$. The first term in the curly brackets in Eq. (22) represents the product of corresponding terms for single boxes [c.f. Eq. (20)]. The second term in the brackets in Eq. (22) can be associated with *nonlinear interference*. It is due to this term that the result from the two-pulse initial condition is not a simple sum of the dynamics originating from each pulse.

The interaction of pulses in the CM system was studied in the paper [9] (see also [24,25]). The main conclusions were the following [9]:

(i) The zeros of $s_{11}(\lambda)$ can be complex with non-zero real parts, even for two *real* initial pulses, i.e. for real $Q_{ja}$ and $Q_{jb}$, and $v_a = v_b = 0$. This means that solitons with non-zero velocities appear. The parameters of the solitons, such as the amplitude and velocity, strongly depend on the parameters of the initial pulses, as well as on the separation distance $L$.

(ii) The number $N_S$ of emerging solitons for some separation distances can be larger then the sum of emerging solitons from each of the two pulses. For fixed parameters of the initial pulses, $N_S$ can vary as $L$ changes.

These conclusions are also valid, in general, for the MM system. Let us analyze some particular cases. For the rest of this section, we take $v_a = v_b = 0$, and $w_a = w_b = 1$, and we consider only the MM system. The procedure is similar to that in Section 3.1. Thus, one solves for the zeros of $s_{11}(\lambda)$, Eq. (22). When they exist, they define the parameters of the emerging solitons. If the initial condition generates no solitons, then Eqs. (18) and (22) can be used for the reconstruction of the asymptotic state of the field.

### 3.2.1. The case $\frac{Q_{1a}}{Q_{2a}} = \frac{Q_{1b}}{Q_{2b}} = \alpha$

Such initial conditions are particular cases of a more general initial condition in the form:

$$q_1(x,0) = \alpha q_2(x,0), \tag{23}$$

where $\alpha$ is a complex constant. Then the vector NLS Eq. (2) reduces to the scalar one for the function $q_1(x,z)$ or $q_2(x,z)$, and another field is found from the relation $q_1(x,z) = \alpha q_2(x,z)$. If $|\alpha| = 1$, then both components propagate as linear waves.

The interaction of solitons in the scalar focusing and defocusing NLS equations is a well-studied problem (see e.g. [26,27]). Usually, the pulses were considered in the form of hyperbolic secants with the amplitudes approximately equal to the inverse widths in dimensionless units [c.f. (15)]. In other words, each pulse was taken to be close to the one-soliton solution. The interaction of pulses that have an arbitrary relation between the amplitude and width, i.e. pulses consisting of several solitons, were considered only recently [24,25]. An application of the IST method to pulses with rectangular shape allows one to analytically solve the problem of the interaction.

### 3.2.2. The case $Q_{1a}^{\star} Q_{1b} = Q_{2a}^{\star} Q_{2b}$

Particular examples of such initial conditions are $Q_{1a} = Q_{2b} = 0$ or $Q_{2a} = Q_{1b} = 0$, which correspond to the interaction of pulses which are initially in different components. In the general case, as follows from Eq. (22), the nonlinear interference term disappears. The parameter $s_{11}(\lambda)$ is now expressed in a factorized form so that the discrete spectrum can easily be found. In fact, for such initial conditions, only one pulse of these two can produce solitons, while the other will dispersively decrease. The number of solitons corresponds to that for a single pulse. If $I_{0a} w^2 < \pi^2/4$ and $I_{0b} w^2 < \pi^2/4$, then the initial condition evolves into dispersive waves. The asymptotic state for such initial conditions can be found from Eqs. (18) and (22).

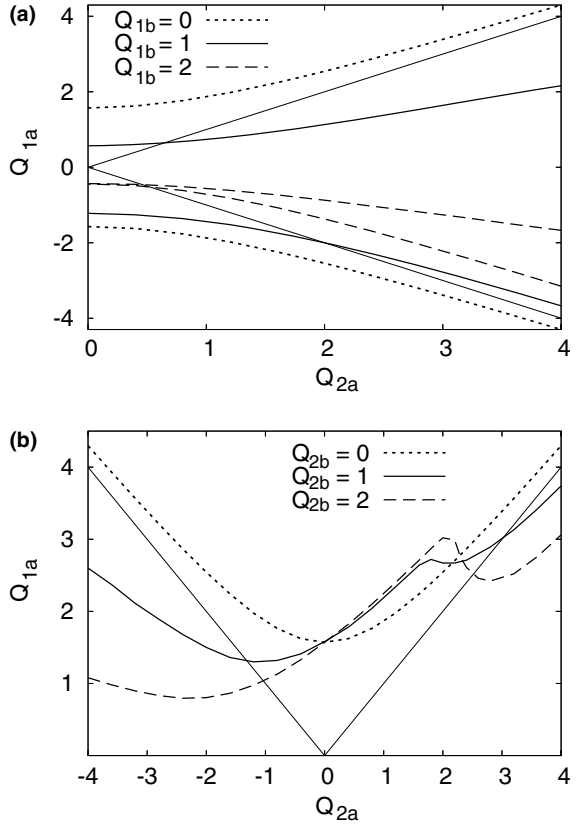


Fig. 2. Thresholds for soliton generation from initial condition (21) with different values of $Q_{1b}$. Parameters are $L = 0$, $w_a = w_b = 1$, (a) $Q_{2b} = 0$, and (b) $Q_{1b} = 0$.

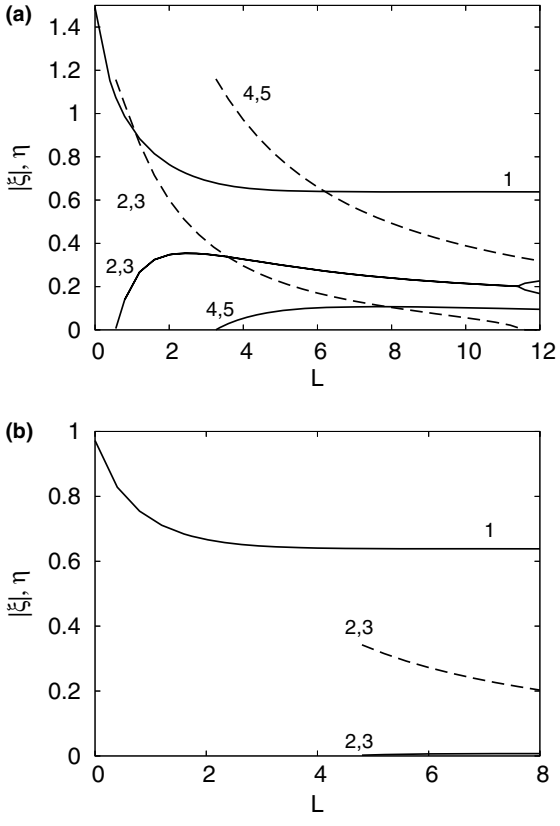


Fig. 3. Eigenvalues $\lambda_n = \xi_n + i\eta_n$ for initial condition (21) as functions of the separation distance. The parameters are $w_a = w_b = 1$, (a) $(Q_{1a}, Q_{2a}) = (2,1)$. Only the first five eigenvalues are shown; (b) $(Q_{1a}, Q_{2a}) = (1,2)$, while $(Q_{1b}, Q_{2b}) = (2,0)$ in both cases. Solid (dashed) lines correspond to $\eta_n$ ($\xi_n$). Numbers near the lines correspond to the number $n$ of the eigenvalue $\lambda_n$.

*3.2.3. The case $Q_{2b} = 0$*

It is difficult to find a simple expression, similar to that in the case of a single pulse (see Section 3.1), for the number of emerging solitons. We have found, computationally, the thresholds for soliton generation by numerically solving the equation $s_{11}(\lambda) = 0$. The result for $L = 0$ in the plane $(Q_{2a}, Q_{1a})$, considering $Q_{1b}$ as a parameter, is presented in Fig. 2a. The non-soliton area is between two lines of the same type. For $Q_{1b} = 0$, the threshold is found from $Q_{1a} = \pm[\pi^2/(4w^2) - |Q_{2a}|^2]^{1/2}$. We also show, as a reference, the lines $Q_{1a} = \pm Q_{2a}$. The plot is symmetric about $Q_{2a} = 0$. One can see that with an increase of $Q_{1b}$, the boundaries approach each other. This is obvious, since the energy of the first (focusing) component increases. For $Q_{1b} = 0$, if $|Q_{1a}|$ is larger than the threshold value, then a single soliton with zero velocity appears. For $Q_{1b} > 0$, a single soliton appears above the upper boundary, while below the lower boundary, a pair of solitons with opposite velocities can appear. A sign change of $Q_{1b}$ results in a sign change of the boundary values.

Let us now consider the dependence of the dynamics on the separation distance $L$. We take the following initial conditions: $(Q_{1a}, Q_{2a}) = (2, 1)$, $(Q_{1b}, Q_{2b}) = (2, 0)$ and $w_a = w_b = 1$. The eigenvalues $\lambda_n = \xi_n + i\eta_n$, found from a numerical solution of Eq. (22), are shown in Fig. 3a. The numbers near the curves correspond to the eigenvalue numbers. Note that $\mathrm{Re}[\lambda_2] = -\mathrm{Re}[\lambda_3]$, $\mathrm{Re}[\lambda_4] = -\mathrm{Re}[\lambda_5]$, etc. Recall that $2\eta_n = (A_{1n}^2 - A_{2n}^2)^{1/2}$ is related to the peak norm of the $n$th soliton [c.f. Eq. (15)], where $A_{1n}$ and $A_{2n}$ are the amplitudes of the field components of the $n$th soliton. Parameter $4\xi_n$ is the velocity of the $n$th soliton. For $L \lesssim 0.56$, only one pure imaginary root exists, $\lambda_1 = i\eta_1$. At $L = 0.56,\ 3.26,\ 6.0,\ 8.8\ldots$ pairs of solitons with opposite velocities appear. We have shown only the first five eigenvalues. At $L \gtrsim 11.5$, $\mathrm{Re}[\lambda_2] = \mathrm{Re}[\lambda_3] = 0$, so that the three pure imaginary eigenvalues give rise to a bound state of three solitons. With an increase in $L$, $\eta_1 \to 0.638$ and $\eta_2 \to 0.248$, which are the eigenvalues of well-separated pulses. All other eigenvalues $\lambda_n$, $n \geqslant 3$, tend to zero at large $L$.

Fig. 3b shows the result for $(Q_{1a}, Q_{2a}) = (1, 2)$ and $(Q_{1b}, Q_{2b}) = (2, 0)$. Only three eigenvalues exist for $0 < L < 8$. Note that the parameters of the $a$-pulse are such that it does not generate solitons, however as a result of the interaction between pulses, a pair of solitons appears. Those solitons have very small amplitudes, but since they

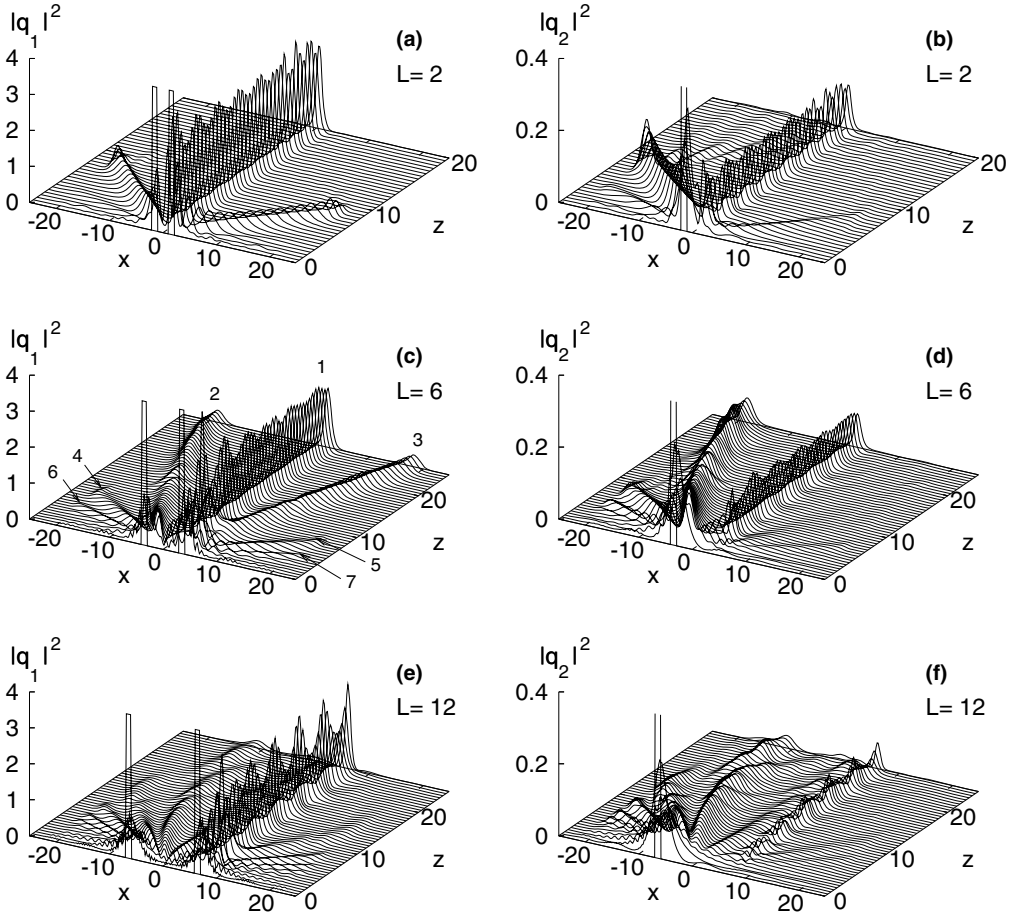


Fig. 4. The evolution of the field components for different separation distances. The initial conditions are the same as in Fig. 3a. (a,b) $L = 2$, (c,d) $L = 6$, and (e,f) $L = 12$. The numbers in (c) indicate the corresponding numbers of the solitons.

correspond to *non-dispersive* packets, they should be taken into account. Of course, for larger values of $Q_{1a}$, the amplitudes of additional solitons will be more appreciable.

The dynamics presented in Fig. 3a has been checked by a direct numerical simulation of the MM system (2). Fig. 4 shows the evolution of the field components for initial conditions corresponding to Fig. 3a at different separation distances. We use a standard split-step method [1] with absorbing boundary conditions. One can see that three solitons exist at $L = 2$ (Figs. 4a and b), where one soliton is static and the other two solitons with smaller amplitudes propagate in opposite directions. The evolution of $q_2$ is obviously asymmetric, because of the asymmetry of the initial condition of that component. The dynamics for $L = 6$ is presented in Figs. 4c and d. One can distinguish one static and three pairs of moving solitons, though the component $q_2$ of some solitons is very small. We recall that $L = 6$ is the threshold where a new pair of solitons appears. Therefore, the asymptotic amplitudes of the sixth and the seventh solitons are zero. As seen from Figs. 4c and d, the amplitudes of these solitons indeed decrease during the propagation in $z$, from 0 to ~5. At $L = 12$ (see Figs. 4e and f), there is the three-soliton solution and also several moving solitons. This is consistent with Fig. 3a. The amplitudes of moving solitons are smaller than those for $L = 2$ and $L = 6$. The amplitude of the static pulse oscillates with large deviations. This is typical for a bound state of several solitons.

Fig. 5 shows the dependence of the peak norm $A_{11}^2 - A_{21}^2$ of the first (largest) soliton on $z$, where $A_{11}$ and $A_{21}$ are the peak amplitudes of the components. Horizontal lines correspond to the asymptotic values (c.f. Fig. 3a). The asymptotic values for $L = 6$ and $L = 12$ are close to each other, so only one line is shown. One can see good agreement between the theory and numerical simulations of Eq. (2). The result for $L = 12$ is unexpected. Although the initial pulses are far from each other, they result in a bound state of three solitons, while for shorter separation distances, only single solitons emerge.

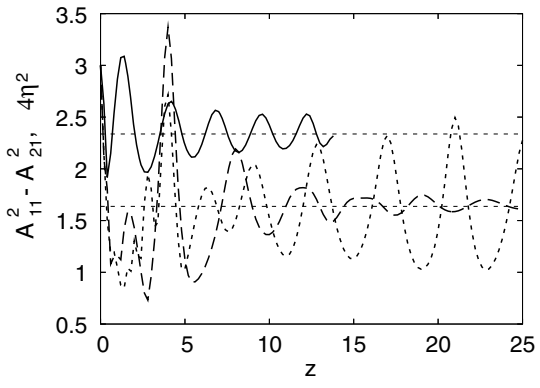


Fig. 5. The dependence of the peak norm $A_{11}^2 - A_{21}^2$ of the largest soliton on $z$ for $L = 2$ (solid line), $L = 6$ (dashed line), and $L = 12$ (dotted line), as found from numerical simulation of Eq. (2). The thin horizontal lines are asymptotic values $4\eta^2$. Initial conditions are the same as in Fig. 3a.

*3.2.4. The case $Q_{1b} = 0$*

The thresholds for soliton generation for this case, when $L = 0$ and $w_a = w_b = 1$, are presented in Fig. 2b. The plot is symmetric about $Q_{1a} = 0$. A change in the sign of $Q_{2b}$ results in a symmetry reflection about $Q_{2a} = 0$. Above the threshold and at $Q_{2a} \lesssim 2$, a single soliton with zero velocity appears, while at $Q_{2a} \gtrsim 2$, two moving solitons appear. This explains the non-monotonic dependence of the threshold near this point. As in the previous case, the non-soliton area decreases with an increase in $Q_{2b}$.

The dependence of the eigenvalues on $L$ is shown in Fig. 6. Let us first consider the following initial condition $(Q_{1a}, Q_{2a}) = (2, 1)$, $(Q_{1b}, Q_{2b}) = (0, 2)$, and $w_a = w_b = 1$ (see Fig. 6a). Only the first four eigenvalues are shown in the figure. At $L \lesssim 6.7$, the eigenvalues $\lambda_1$ and $\lambda_2$ correspond to oppositely moving solitons with the same amplitude. At $L \gtrsim 6.7$, the real parts of the eigenvalues become zero, so that a bound state of two solitons is formed. At large $L$, $\lambda_1 \to 0.248$, which corresponds to a soliton emerging from an $a$-pulse, while all the other eigenvalues tends to zero.

The dependence of the eigenvalues for $(Q_{1a}, Q_{2a}) = (1, 2)$, $(Q_{1b}, Q_{2b}) = (0, 2)$ and $w_a = w_b = 1$ is presented in Fig. 6b. Note that neither the $a$-pulse nor the $b$-pulse, when considered separately, results in solitons. However, the

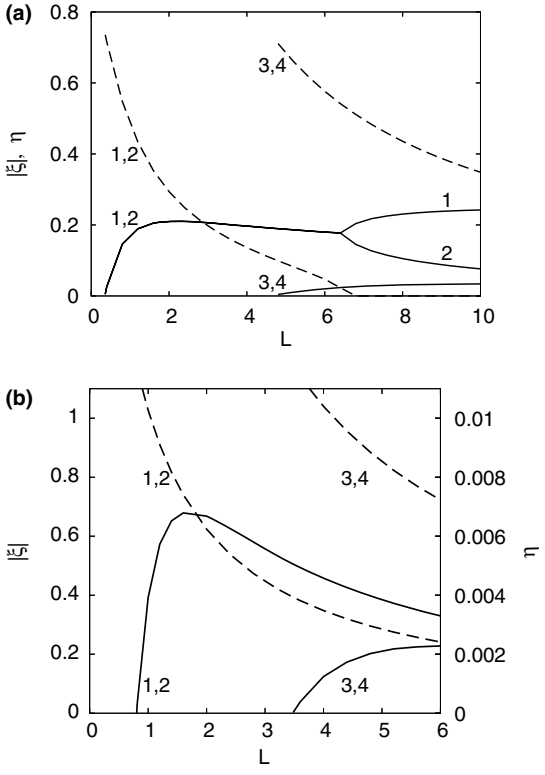


Fig. 6. Eigenvalues $\lambda_n = \xi_n + i\eta_n$ as functions of the separation distance. The parameters are $w_a = w_b = 1$. (a) $(Q_{1a}, Q_{2a}) = (2, 1)$; (b) $(Q_{1a}, Q_{2a}) = (1, 2)$, while $(Q_{1b}, Q_{2b}) = (0, 2)$ in both cases. Solid (dashed) lines correspond to $\eta_n$ ($\xi_n$).

interaction between them produces the solitons, though they have very small amplitudes.

As follows from Fig. 2, the variation of the field in the second component changes the parameters of the emerging solitons, and therefore the interaction of pulses. One can see from Figs. 3 and 6 that bifurcations occur for separation distances $L \sim 2$–$10$. For the system parameters mentioned at the end of Section 3.1, this corresponds to $L \sim 50$–$500$ μm.

## 4. Conclusions

We have considered the evolution of rectangular pulses in the modified Manakov system, Eq. (2) with $\sigma = -1$. The study is based on the inverse scattering transform method. Namely, we have solved the direct scattering problem and have shown how the asymptotic state of the system can be found from the scattering data. We have demonstrated that both the parameters of solitons and the asymptotics of the field in the non-soliton regime can be recovered from the coefficient $s_{11}(\lambda)$. We have considered single-pulse and two-pulse initial conditions. We found that the case of the single-pulse initial condition reduces to the scalar (focusing or defocusing) form. The interaction of two pulses separated by an intermediate distance may result in the appearance of additional moving solitons and in the formation of bound states of several solitons.

In contrast to the CM system, the MM model is not symmetric relative to the transformation $q_1 \leftrightarrow q_2$. Therefore, the dynamics strongly depends on the initial distribution of the energy between the components. The propagation of pulses in the MM system can be similar to that in linear, focusing or defocusing media. We have shown that by changing the field in the second component, one can control the parameters of solitons emerging from a single pulse. For large initial values of $|Q_2|$, it is even possible to suppress the creation of solitons, so that the initial pulse decays dispersively. As has been shown in Section 3.2, one can also change the interaction of pulses by varying the field in the second component. Therefore, such a two-component scheme can be used for data manipulation. The first component plays the role of a data carrier, while the second component is used as a control of the signal. The distance between adjacent beams should be larger than $\sim 10 w_{\text{in}}$ in order to avoid the creation of additional beams.

It can also be interesting to study the dynamics of waves with different boundary conditions, for example with non-zero values of $q_2$ at $x \to \pm\infty$. In this case, a basic solution of Eq. (2) is represented as a pair of bright and dark solitons. However, such a case requires the reformulation of the inverse scattering method and separate studies.

## Acknowledgments

This work was funded by the Australian Research Council. E.N.T. thank Uzbek Academy of Sciences for partial support of this study (Grant AN RUz N 17-04). The authors are grateful to B.B. Baizakov for useful discussions and to A. Ankiewicz for a critical reading of the manuscript.

## References

[1] See e.g.: N. Akhmediev, A. Ankiewicz, Solitons: Nonlinear Pulses and Beams, Chapman & Hall, London, 1997;
G.P. Agrawal, Nonlinear Fiber Optics, Academic Press, London, 1989.
[2] S.V. Manakov, Zh. Eksp. Teor. Fiz. 65 (1973) 505 [Sov. Phys. JETP 38 (1974) 248].
[3] U. Lindner, V. Fedyanin, Phys. Stat. Sol. (B) 89 (1978) 123.
[4] Y. Chen, H.A. Haus, Opt. Lett. 25 (2000) 290.
[5] V.P. Mineev, Zh. Eksp. Teor. Fiz. 67 (1974) 263 [Sov. Phys. JETP 40 (1974) 132].
[6] Yu.A. Nepomnyashchii, Zh. Eksp. Teor. Fiz. 70 (1976) 1070 [Sov. Phys. JETP 43 (1976) 559].
[7] V.E. Zakharov, E.I. Schulman, Physica D 4 (1982) 270.
[8] D.J. Kaup, B.A. Malomed, Phys. Rev. A 48 (1993) 599.
[9] F. Kh. Abdullaev, E.N. Tsoy, Physica D 161 (2002) 67.
[10] V.G. Makhankov, N.V. Makhaldiani, O.K. Pashaev, Phys. Lett. A 81 (1981) 161;
V.G. Makhankov, O.K. Pashaev, Teor. Mat. Fiz. 53 (1982) 55.
[11] T. Kanna, E.N. Tsoy, N. Akhmediev, Phys. Lett. A 330 (2004) 224.
[12] A.G. Kalocsai, J.W. Haus, Phys. Rev. E 52 (1995) 3166.
[13] H.S. Eisenberg, Y. Silberberg, R. Morandotti, A.R. Boyd, J.S. Aitchison, Phys. Rev. Lett. 81 (1998) 3383;
J. Meier, J. Hudock, D. Christodoulides, G. Stegeman, Y. Silberberg, R. Morandotti, J.S. Aitchison, Phys. Rev. Lett. 91 (2003) 143907.
[14] S.A. Darmanyan, A. Kobyakov, E. Schmidt, F. Lederer, Phys. Rev. E 57 (1998) 3520.
[15] J. Hudock, P.G. Kevrekidis, B.A. Malomed, D.N. Christodoulides, Phys. Rev. E 67 (2003) 056618.
[16] A.A. Sukhorukov, Yu. S. Kivshar, Phys. Rev. Lett. 91 (2003) 113902.
[17] B.P. Anderson, M.A. Kasevich, Science 282 (1998) 1686.
[18] B. Eiermann, P. Treutlein, Th. Anker, M. Albiez, M. Taglieber, K.P. Marzlin, M.K. Oberthaler, Phys. Rev. Lett. 91 (2003) 060402;
B. Eiermann, Th. Anker, M. Albiez, M. Taglieber, P. Treutlein, K.P. Marzlin, M.K. Oberthaler, Phys. Rev. Lett. 92 (2004) 230401.
[19] O. Zobay, S. Pötting, P. Meystre, E.M. Wright, Phys. Rev. A 59 (1999) 643;
S. Pötting, O. Zobay, P. Meystre, E.M. Wright, J. Mod. Opt. 47 (2000) 2653.
[20] M. Trippenbach, K. Goral, K. Rzazewski, B. Malomed, Y.B. Band, J. Phys. B 33 (2000) 4017.
[21] P.G. Kevrekidis, B.A. Malomed, D.J. Frantzeskakis, A.R. Bishop, Phys. Rev. E 67 (2003) 036614.
[22] M.J. Ablowitz, B. Prinari, A.D. Trubach, Discrete and Continuous Nonlinear Schrödinger Systems, Cambridge University Press, 2004.
[23] V.E. Zakharov, S.V. Manakov, S.P. Novikov, L.P. Pitaevsky, Theory of Solitons, Nauka, Moscow, 1980;
M.J. Ablowitz, H. Segur, Solitons and the Inverse Scattering Transform, SIAM, Philadelphia, 1981.
[24] W.M. Liu, B. Wu, Q. Niu, Phys. Rev. Lett. 84 (2000) 2294.
[25] E.N. Tsoy, F. Kh. Abdullaev, Phys. Rev. E 67 (2003) 056610.
[26] C. Desem, P.L. Chu, in: J.R. Taylor (Ed.), Optical Soliton – Theory and Experiment, Cambridge University Press, 1992, p. 107.
[27] A. Hasegawa, Yu. Kodama, Solitons in Optical Communications, Clarendon Press, Oxford, 1995 (Chapter 9).